CrystEngComm

COMMUNICATION

View Article Online
View Journal | View Issue

Controllable growth of a forest of silver nanowires and their field emission properties†

Changlong Jiang,*[a] Shengjun Liu,[a] Xiaochun Chen[b] and Shaoming Yu*[b]

Cite this: *CrystEngComm*, 2014, **16**, 8646

Received 10th May 2014,
Accepted 24th July 2014

DOI: 10.1039/c4ce00977k

www.rsc.org/crystengcomm

The development and innovation of strategies for the fabrication of oriented nanostructures has been among the hot research topics in the field of nanoscience because of the novel properties of these nano-arrays, that differ drastically from their bulk counterparts, and their potential applications in many areas including the chemical, physical, biological and engineering fields. Herein, we have demonstrated an extremely simple procedure for the fabrication of a forest of oriented silver nanowires at ambient temperature in aqueous solution without a hard template. The oriented silver nanowire arrays exhibit better field emission performance than that of a single nanowire or non-oriented nanowires. By variation of the experimental parameters, the diameter and length of the oriented Ag nanowires can be tuned accordingly. The successful fabrication of a forest of the oriented nanowires under mild conditions without a template not only provides an efficient route to selectively control the preparation of oriented nano-arrays, but also provides new insights into the underlying surfactant-mediated mechanism of nano- and micro-architectures. This strategy might be extended to fabricate other metal and semiconductor nanocrystal arrays and widen their potential applications in many fields.

1. Introduction

One-dimensional (1D) nanostructures (such as wires, rods, tubes, and belts) have been the focus of extensive research in recent years due to their potential applications in fabricating nanoscale electronic, optoelectronic, and sensing devices.[1] More recently, many efforts have been devoted to the controlled synthesis and assembly of metal nanowires owing to their promising use as interconnects or active components in fabricating nanodevices and their important roles in probing a variety of physical phenomena.[2] Field emission (FE), also known as cold emission, is one of the main features of nanostructures and has been extensively studied for its importance in both fundamental research and device applications.[3] This phenomenon is highly dependent on both the properties of the material and the shape of the particular cathode, so that higher aspect ratios (height/tip radius) produce higher field-emission currents at a lower applied electric field. In recent years, high-performance field emitters have attracted a lot of attention because of their wide applications in FE-based vacuum microelectronic devices, such as field-emission displays, microwaves, and amplifiers, where a higher current density, larger field-enhancement factor, and lower turn-on field and threshold field are needed.[4] In particular, there are several merits to using metal nanowires as field-emission (FE) tips, compared to semiconducting nanowires such as ZnO and GaN; a metallic nanowire tip would be advantageous in terms of electric conductivity, which significantly lowers the driving voltage for field emission.[5] Some FE tips based on copper, gold, and tungsten nanowires with appreciable emission performances have been fabricated.[6] Field-emission devices with low threshold voltages are potentially useful as electron emitters in flat panel displays. In addition, one-dimensional nanostructures are also ideal candidates for achieving high field emission (FE) current density at a low electric field because of their high aspect ratio, low work function, and high mechanical stability and conductivity.[7] Accordingly, in the past few years, intensive research efforts have been devoted to the design and fabrication of cold cathode electron emitters.[8]

The controlled synthesis and applications of silver nanowires have received much attention in the past few years because bulk silver exhibits the highest electrical and thermal conductivity among all metals.[9] Silver has also been used in a rich variety of commercial applications including surface plasmonics, surface-enhanced Raman scattering (SERS), as well as chemical and biological sensing.[10] The performance

[a] *Institute of Intelligent Machines, Chinese Academy of Sciences, Hefei, Anhui, 230031, China. E-mail: cljiang@iim.ac.cn*
[b] *School of Chemical Engineering, Hefei University of Technology and Anhui Key Laboratory of Controllable Chemical Reaction & Material Chemical Engineering, Hefei 230009, Anhui, China. E-mail: shmyu@hfut.edu.cn*

† Electronic supplementary information (ESI) available. See DOI: 10.1039/c4ce00977k

of silver in these applications can be enhanced by processing silver into 1D nanostructures which have well-controlled dimensions, a high aspect ratio, and are even uniformly oriented.[11] The successful alignment and patterning of the nanowires can significantly impact many areas such as nanoscale electronics, optoelectronics, and molecular sensing.[12] One of the powerful and now extensively used methods for synthesizing oriented 1D nanostructures relies on solid-state templates, such as carbon nanotubes, porous polycarbonate and alumina membranes, and mesoporous silica, and electrochemistry to control the diameter and length of such structures.[13] Because this process requires the removal of the template, it is desirable to develop a simple and direct method to prepare oriented 1D nanostructures to avoid the removal of the template after the synthesis. Herein, we report a one-pot, templateless, facile aqueous approach to prepare a forest of oriented silver nanowires at room temperature. The diameter and length of the silver nanowires in the system can be tuned by varying the experimental parameters. The forest of silver nanowire arrays exhibits better field emission (FE) performance than that of a single nanowire or non-oriented nanowires, which can be attributed to their good orientation, uniform size and high density.

2. Experimental section

2.1 Materials

All chemicals were of analytical grade and used without further purification. Cetyltrimethylammonium bromide (CTAB), silver nitrate ($AgNO_3$) and dodecylamine (DA) were purchased from Sigma-Aldrich. Ultrapure water (18.2 MΩ cm) was produced using a Millipore water purification system.

2.2 Synthesis of the oriented Ag nanowire arrays on a Si substrate

To prepare the oriented Ag nanowire arrays on a Si wafer, a Si wafer (about 0.6 cm^2) was pretreated with O_2 plasma for 10 minutes to improve its surface hydrophilicity. The wafer was then functionalized with an amino group by reacting with a solution of (3-aminopropyl)triethoxysilane (APTES, 5 mM) for 2 h. Meanwhile, $AgNO_3$ (400 mg, 2.35 mmol), dodecylamine (DA, 120 μL, 0.522 mmol), and cetyltrimethylammonium bromide (CTAB, 200 mg, 0.55 mmol) were mixed in 10 mL distilled water to give a solution under magnetic stirring for 1 minute. The functionalized wafer was then immersed in the above reaction solution for 24 h at room temperature (25 °C) to ensure adsorption of the Ag seeds and further nanowire arrays formation. Finally, the wafer was rinsed several times with ethanol to remove any impurities and dried in air. The samples were then collected for further characterization.

2.3 Instruments

Field-emission scanning electron microscopy (FE-SEM) images were obtained using a JEOL JSM 6701 microscope, operating at 10 A and 5 kV, by mounting the sample on carbon film. Transmission electron microscopy (TEM) was performed with a JEOL 3010 instrument. When preparing the sample, the product was suspended in ethanol by ultrasonic dispersion without further purification. The ethanol suspension of the product was then dropped on a copper grid coated with amorphous carbon film for TEM characterization. The crystallographic phase of the sample was determined by powder XRD on a Siemens D5005 X-ray diffractometer with Cu Kα radiation (λ = 1.5406 Å) at a scan rate of 0.01° s^{-1} at 40 kV/40 mA in the 2θ range from 10° to 80°. Field emission measurements for the oriented Ag nanowire arrays were conducted in a vacuum chamber at a pressure of 8×10^{-6} Torr at room temperature.

3. Results and discussion

The current synthesis of the Ag oriented nanowire arrays was based on a surfactant-mediated method in aqueous solution at room temperature. Field-emission scanning electron microscopy (FE-SEM) was used to check the surface morphology of the as-prepared Ag sample. Fig. 1a presents a low magnification

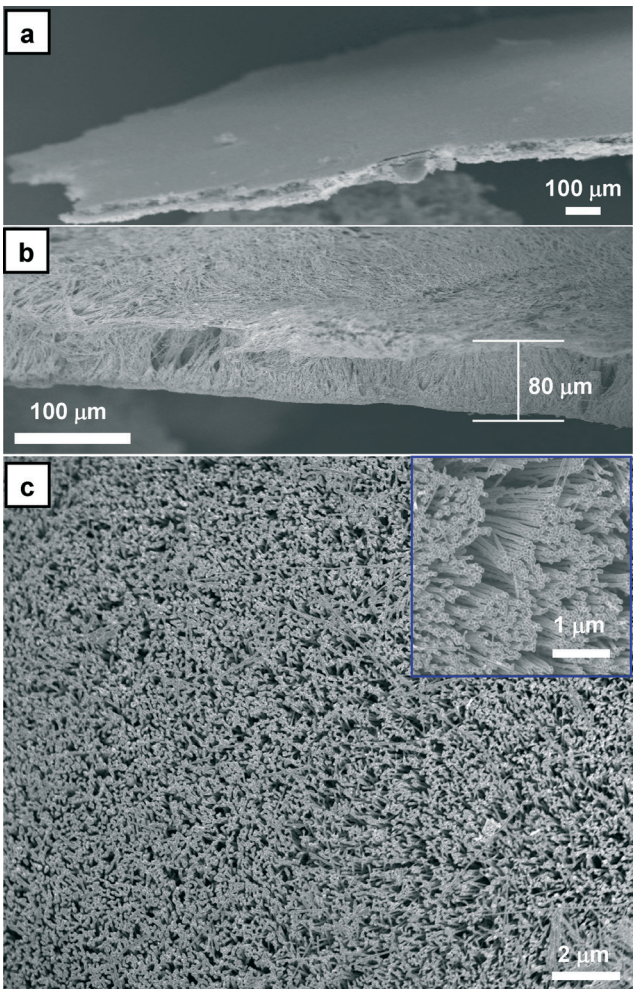

Fig. 1 FE-SEM images of the Ag oriented nanowire arrays. a) Low magnification image of the as-prepared Ag oriented nanowire array thin film. b) SEM images of the Ag nanowire arrays. c) A top-view image of the Ag oriented nanowire arrays; the inset is a high magnification, top-view SEM image.

image of the obtained Ag oriented nanowire array thin film with a smooth surface morphology. The oriented texture of the sample can be better seen from the cross-section pattern in Fig. 1b, and the silver oriented nanowires have a uniform diameter and a length of about 80 μm. The top-view SEM image (Fig. 1c) reveals that most nanowires are oriented and are of uniform diameter and length, and the high magnification top-view pattern (inset in Fig. 1c) further displays their uniformity.

As shown in Fig. 2, the as-obtained oriented Ag nanowires have a uniform size and morphology. Fig. 2a is a low magnification top-view image of the oriented nanowire arrays. The oriented texture of the sample can be better seen from the top-view pattern in Fig. 2b; all the nanowires have a uniform size and are vertically aligned, and the high magnification version of the top-view image (inset in Fig. 2b) reveals that the Ag nanowires have a broad head on the top. A high magnification image of the cross-section (Fig. 2c) reveals that most of the nanowires are oriented and have a uniform diameter and length. The Ag nanowires are about 100 nm in diameter and have a uniform length of about 80 μm. This result indicates that oriented metal nano-arrays can be prepared *via* a surfactant-mediated strategy under mild conditions.

The phase of the as-prepared sample was determined by X-ray powder diffraction (XRD) and all of the diffraction peaks shown in Fig. 3a could be indexed to pure face-centered cubic Ag (Joint Committee on Powder Diffraction Standards (JCPDS) card no. 04-0783). It is worth noting that the ratio between the intensities of the (111) and (200) diffractions peaks was higher than the conventional value (4.4 verse 2.5), indicating that the obtained nanowires were abundant in {111} facets, and thus their {111} planes tended to be preferentially oriented. The TEM pattern of the Ag oriented nanowires (Fig. 3b) reveals that the nanowires have a uniform diameter of about 100 nm, in agreement with the results of SEM in Fig. 1. A single silver nanowire is presented in Fig. 3c. The single-crystalline nature of the oriented Ag nanowires is confirmed by the corresponding fast-Fourier transformation (FFT) pattern along the constituent nanowire (inset in Fig. 3c). The FFT pattern reveals that the nanowire has a cubic crystal structure which grows along the [011] direction. The high-resolution TEM image shown in Fig. 3d exhibits clear lattice fringes with a *d* spacing of about 0.24 nm, which agrees well with the *d* (111) spacing for fcc Ag, confirming that the nanowires are single crystals of cubic silver with [011] as the growth direction.

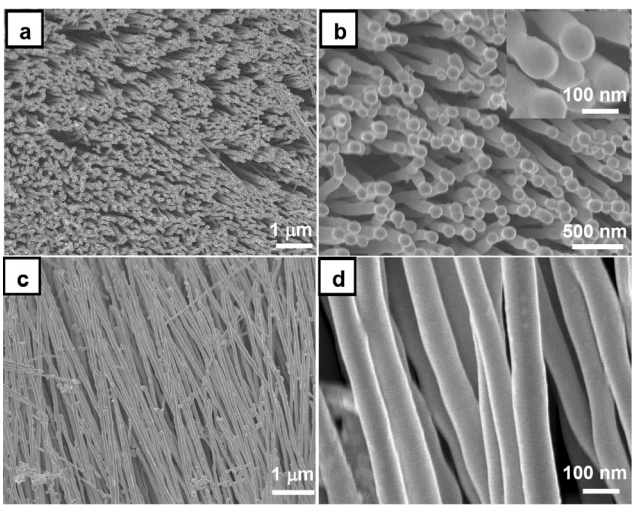

Fig. 2 FE-SEM images of the Ag oriented nanowire arrays. a) Low magnification image (top-view) of the as-prepared Ag oriented nanowire arrays. b) A top-view image of the Ag oriented nanowire arrays; the inset is a high magnification, top-view SEM image. c) Low magnification image (cross-section) of the Ag oriented nanowire arrays. d) A high magnification, cross-section image of the Ag oriented nanowire arrays.

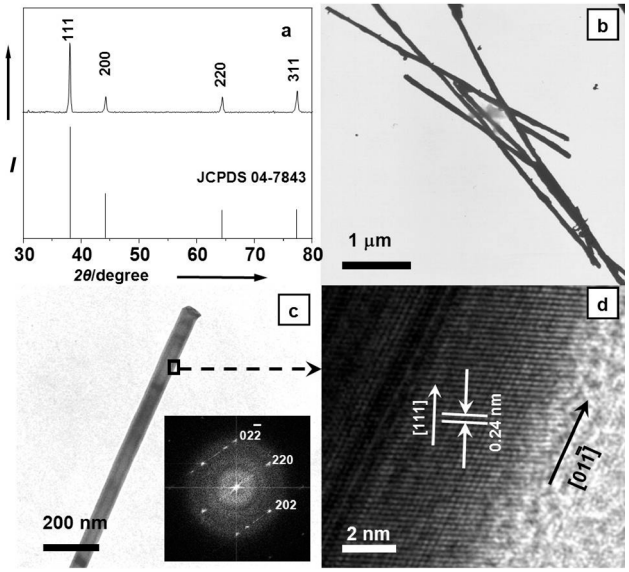

Fig. 3 Characterization of the Ag ordered nanowire arrays. a) XRD pattern of the nanowire arrays. b) and c) TEM images of the Ag ordered nanowire arrays; the inset shows the corresponding FFT pattern of the single nanowire in Fig. 2c. d) HRTEM image of the area indicated in Fig. 2c.

To facilitate studies on the evolution of the morphology of the silver sample, several adjustments were made to the experimental parameters. The length of the nanowires increases with an increase in the reaction time (Fig. 4). After a short time (6 h), the obtained oriented nanowire arrays are only 10 μm in length. After increasing the time in the reaction system at room temperature to 12 h, the length of the nanowires reaches 30 μm and when the reaction is maintained for 28 h, the obtained sample has a length of about 80 μm. The final silver oriented nanowires have lengths of up to 200 μm if kept in the reaction system for two days, but the obtained long nanowire arrays can no longer retain their vertical alignment on the top. The reaction temperature might play an important role in the control of the diameter of the oriented silver nanowire arrays (Fig. S1†). When the reaction temperature is enhanced from room temperature (25 °C) to 40 °C, the diameter increases from 100 nm to 200 nm. The nanowires are 250 nm in diameter when the

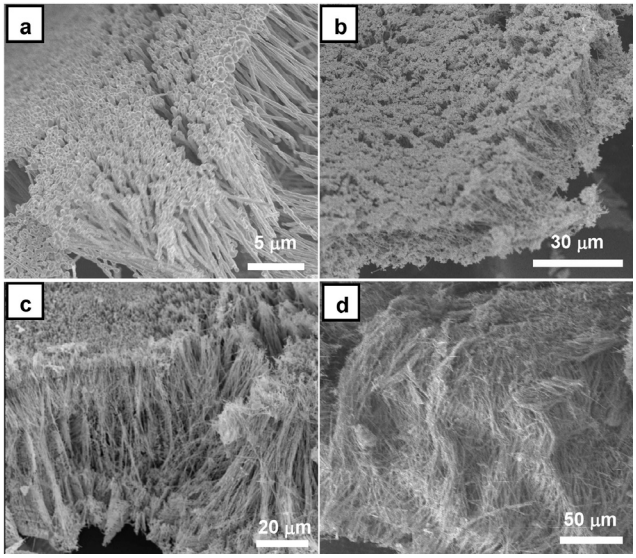

Fig. 4 SEM images of the Ag oriented nanowire arrays obtained with different lengths at room temperature. a) 10 μm when prepared for 6 h; b) 30 μm when prepared for 12 h; c) 80 μm when prepared for 28 h; d) 200 μm when prepared for 48 h.

temperature is set to 50 °C. The diameters of the Ag nanowires are about 300 nm and 400 nm when the reaction is performed at 70 °C and 90 °C, respectively. This could be attributed to a larger crystal growth rate at higher temperature.

It is worth mentioning that a static condition without stirring is required for the formation of the ideal silver oriented nanowire arrays in the current synthesis. If stirring is conducted throughout the process, only random nanowires are obtained, suggesting that the convection induced by stirring considerably disturbs the final formation of the oriented nanowire arrays. To further understand the detailed formation of the intriguing oriented silver nanowire arrays in aqueous solution under an ambient atmosphere, we performed related experiments at various time intervals as shown in Fig. S2.† At the initial stage (10 min), only a layer of silver nanoparticles had formed. When the reaction continued for 1 h, very short rod-like silver nanoparticles could be seen, as shown in Fig. S2c.† The sample synthesized at 3 h took the shape of oriented silver nanorods, as shown in Fig. S2d.† Increasing the growth time to 12 h and 24 h resulted in the formation of oriented silver nanowires with lengths of 30 μm and 60 μm, respectively.

Controlling where and how nanocrystals grow is of fundamental importance in nanoscience and nanotechnology. In solution, such control is often realized by exploiting the facet-specific binding of surface ligands, so that preferred growth of certain facets determines the shape of the nanocrystals. Surfactants have been widely employed in the controlled synthesis of inorganic nanostructures.[14] Herein, we also investigated the influence of the surfactant on the morphological evolution of the silver samples. The results indicated that a sufficient concentration of the surfactant (CTAB) was vital for the final formation of the silver oriented nanowire arrays (Fig. S3†). In the absence of the surfactant, only silver particles were obtained. The addition of 15 mM CTAB promoted the formation of a few nanowires in the final sample. A large number of nanowires were formed on increasing the concentration of CTAB to 35 mM. A further increase of the concentration to 55 mM led to oriented nanowire arrays. The synthetic solution became more viscid at a higher CTAB concentration (100 mM) and the resultant silver sample was anomalistic plates instead of nanowires. This indicated that a high enough CTAB concentration was required for the nucleation and 1D growth of silver oriented nanowires but excessive CTAB would considerably inhibit the formation of silver nanowires.

The obtained results indicated that the oriented silver nanowire arrays might be formed through a surfactant-mediated growth process. In the current synthesis, the CTAB surfactant could play multiple roles in the formation of the oriented silver nanowire arrays. When the surfactant concentration reaches a critical value C (critical micellization concentration, CMC), micellization of the surfactant occurs, resulting in the formation of insoluble surfactant complexes. In the current case, the concentration (55 mM) is higher than the CMC value of CTAB in aqueous solution (1.1 mM), therefore insoluble micelle complexes form in the reaction solution, which might serve as "soft templates" for the formation of the oriented silver nanowire arrays in an ambient environment.[15] When crystal growth from the nuclei proceeds through directed diffusion of the primary silver particles/clusters as well as the Ag^{+}–CTAB aggregates, the CTAB molecules could act as efficient capping agents to kinetically control the growth rates of various faces of the silver seeds, leading to highly anisotropic growth of the silver nanocrystals. The possible formation mechanism of the oriented nanowire arrays is shown in Scheme 1.

The FE (field emission) properties of the oriented Ag nanowire arrays were investigated. The FE current density as a function of the macroscopic electric field of the oriented nanowire arrays is shown in Fig. 5a. A turn-on field of 3.4 V μm^{-1} was obtained based on the definition for the field to produce an emission current density of 0.08 mA cm^{-2} with a threshold voltage as low as 50 V. The emission current density reached 1 mA cm^{-2} at an applied field of 5.5 V μm^{-1}. The

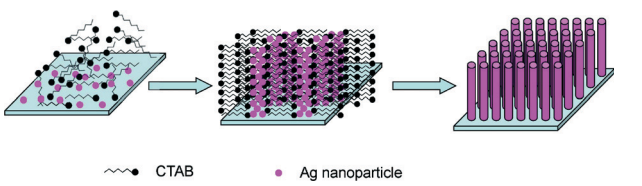

Scheme 1 A schematic illustration of oriented silver nanowire arrays growth: the Ag nanoparticle seeds were formed on the Si substrate and CTAB insoluble micelle complexes in the initial stage, and CTAB insoluble micelle complexes self-formed rod-like micelles along the process; the CTAB rod-like micelles served as soft template for the growth of nanowires from nanoparticle seeds, and finally the Ag nanowire arrays were formed in the Si substrate.

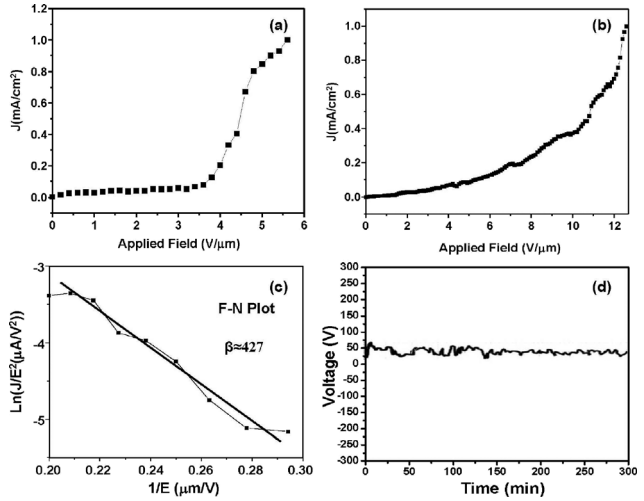

Fig. 5 Field emission properties of the Ag oriented nanowire arrays. FE current density of (a) the oriented Ag nanowire arrays and (b) a single Ag nanowire as a function of the applied electric field; (c) Fowler–Nordheim (F–N) plot of the oriented Ag nanowire arrays; (d) field emission current stability of the oriented nanowire arrays.

plot shown in Fig. 5b, for a single Ag nanowire, does not display typical field emission properties. The FE current density increased to a maximum of 0.98 mA cm^{-2} at an applied field of 12 V μm^{-1} and the nanowire was then burnt. We also tested the FE for non-oriented Ag nanowires, which resulted in no detection of FE properties. Generally, it is well agreed that field emission mainly depends on the tip morphology and the density of the nanostructures. In this case, compared to the single nanowire or non-oriented nanowires, the oriented nanowire arrays exhibit better FE performance which can be attributed to their good orientation, uniform size and high density.[16]

To analyze the field emission properties of the oriented Ag nanowire arrays, a Fowler–Nordheim (F–N) plot was used. The equation can be expressed as:

$$J = A\left(\frac{\beta^2 V^2}{\phi d^2}\right)\exp\left(-\frac{B\phi^{3/2}d}{\beta V}\right),$$

where J is the current density (μA μm^{-2}), A = 1.4 and B = 6440 are constants, ϕ is the work function (eV), d is the distance (μm) between the anode and the cathode, and V is the applied voltage (V). Assuming that the work function of Ag is 3.7 eV, the field enhancement factor, β, is estimated to be 427. Fig. 5c shows a Fowler–Nordheim (F–N) plot of the oriented Ag nanowire arrays. The linear relationship of $1/E$ and $\ln(J/E^2)$ indicates that the field emission behavior of the nanowire arrays fits the F–N mechanism. This β value reflects the degree of FE enhancement of the tip shape on a planar surface. It is dependent on the geometry of the nanowires, the crystal structure, and the density of emitting points. In comparison to a single Ag nanowire and non-oriented nanowires, the oriented Ag nanowire arrays exhibit good field emission and can serve as candidates for emitters in field emission applications. We also checked the FE stability of the Ag oriented nanowire arrays, as shown in Fig. 5d, which proves the stability of the Ag FE emitters.

4. Conclusion

In conclusion, we have demonstrated an extremely simple procedure for the fabrication of a forest of oriented silver nanowires at ambient temperature in aqueous solution without a hard template. The oriented silver nanowire arrays exhibit better FE performance than that of a single nanowire or non-oriented nanowires. By variation of the experimental parameters the diameter and length of the oriented Ag nanowires can be tuned accordingly. The successful fabrication of a forest of oriented nanowires under mild conditions without a template not only provides an efficient route to selectively control the preparation of oriented nano-arrays, but also provides new insights into the underlying surfactant-mediated mechanism of nano- and micro-architectures. This strategy might be extended to fabricate other metal and semiconductor nanocrystal arrays and widen their potential applications in many fields.

Acknowledgements

This work was supported by the National Science & Technology Pillar Program (grant 2012BAJ24B02) and the Natural Science Foundation of China (no. 21371174).

Notes and references

1 (*a*) C. L. Jiang, F. Wang, N. Q. Wu and X. G. Liu, *Adv. Mater.*, 2008, **20**, 4826; (*b*) J. Kong, H. T. Soh, A. M. Cassell, C. F. Quate and H. Dai, *Nature*, 1995, **267**, 222; (*c*) C. L. Jiang, Y. B. Han, S. J. Liu and Z. P. Zhang, *CrystEngComm*, 2014, **16**, 952; (*d*) S. Frank, P. Poncharal, Z. L. Wang and W. A. de Heer, *Science*, 1998, **280**, 1744.

2 (*a*) Y. Xia, P. Yang, Y. Sun, Y. Wu, B. Gate, Y. Yin, F. Kim and H. Yan, *Adv. Mater.*, 2003, **15**, 353; (*b*) J. Hu, T. W. Odom and C. M. Lieber, *Acc. Chem. Res.*, 1999, **32**, 435; (*c*) Y. Cui, Q. Wei, H. Park and C. M. Lieber, *Science*, 2001, **293**, 1289; (*d*) M. A. El-Sayed, *Acc. Chem. Res.*, 2001, **34**, 257; (*e*) C. L. Jiang, S. Ranjit, Z. Y. Duan, Y. L. Zhong, K. P. Loh, C. Zhang and X. G. Liu, *Nanoscale*, 2009, **1**, 391.

3 (*a*) T. Y. Zhai, L. Li, Y. Ma, M. Y. Liao, X. Wang, X. S. Fang, J. N. Yao, Y. Babdo and D. Golberg, *Chem. Soc. Rev.*, 2011, **40**, 2986; (*b*) U. K. Gautam, L. S. Panchakarla, B. Dierre, X. S. Fang, Y. Bando, T. Sekiguchi, A. Govindaraj, D. Golberg and C. N. R. Rao, *Adv. Funct. Mater.*, 2009, **19**, 131.

4 (*a*) X. S. Fang, Y. Bando, U. K. Gautam, C. Ye and D. Golberg, *J. Mater. Chem.*, 2008, **18**, 509; (*b*) T. Y. Zhai, X. S. Fang, Y. Bando, Q. Liao, X. J. Xu, H. B. Zeng, Y. Ma, J. N. Yao and D. Golberg, *ACS Nano*, 2009, **3**, 949; (*c*) J. J. Ding, X. B. Yan, J. Li, B. S. Shen, J. Yang, J. T. Chen and Q. J. Xue, *ACS Appl. Mater. Interfaces*, 2011, **3**, 4299.

5 (*a*) C. J. Lee, T. J. Lee, S. C. Lyu, Y. Zhang, H. Ruh and H. J. Lee, *Appl. Phys. Lett.*, 2002, **81**, 3648; (*b*) B. L. Ward,

O.-H. Nam, J. D. Hartman, S. L. English, B. L. McCarson, R. Schlsser, Z. Sitar, R. F. Davis and R. J. Nemanich, *J. Appl. Phys.*, 1998, **84**, 5238.

6 (*a*) D. N. Davydov, P. A. Sattari, D. Almawlawi, A. Osika and T. L. Haslett, *J. Appl. Phys.*, 1999, **86**, 3983; (*b*) Y. H. Lee, C.-H. Choi, Y. T. Jang, E.-K. Kim, N.-K. Min and J.-H. Ahn, *Appl. Phys. Lett.*, 2002, **81**, 745; (*c*) G. M. Zhou, R. Emmanuel, H. W. Liu, W. M. Liu, S. M. Hou, Y. Z. Kui and Z. Q. Xue, *Chin. Phys. Lett.*, 2002, **19**, 1016.

7 (*a*) M. Ahmad and J. Zhu, *J. Mater. Chem.*, 2011, **21**, 599; (*b*) W. A. De Heer, A. Chatelain and D. A. Ugarte, *Science*, 1995, **270**, 1179; (*c*) N. Pan, H. Xue, M. Yu, X. Cui, X. Wang, J. G. Hou, J. Huang and S. Z. Deng, *Nanotechnology*, 2010, **21**, 225707.

8 (*a*) D. E. Engelsen, *Phys. Procedia*, 2008, **1**, 355; (*b*) E. Stratakis, R. Giorgi, M. Barberoglou, T. Dikonimos, E. Salernitano, N. Lisi and E. Kymakis, *Appl. Phys. Lett.*, 2010, **96**, 043110; (*c*) A. Jha, U. K. Ghorai, D. Banerjee, S. Mukherjee and K. K. Chattopadhyay, *RSC Adv.*, 2013, **3**, 1227.

9 (*a*) S. Nam, H. W. Cho, S. Lim, D. Kim, H. Kim and B. J. Sung, *ACS Nano*, 2013, **7**, 851; (*b*) B. H. Hong, S. C. Bae, C. W. Lee, S. Jeong and K. S. Kim, *Science*, 2001, **294**, 348; (*c*) P. Mohanty, I. Yoon, T. Kang, K. Seo, K. S. K. Varadwaj, W. Choi, Q.-H. Park, J. P. Ahn, Y. D. Suh, H. Ihee and B. Kim, *J. Am. Chem. Soc.*, 2007, **129**, 9576; (*d*) Y. Sun, B. Mayers, T. Herricks and Y. Xia, *Nano Lett.*, 2003, **3**, 955; (*e*) C. L. Jiang, S. J. Liu and Y. B. Han, *CrystEngComm*, 2013, **15**, 7564.

10 (*a*) M. Chen, C. J. Wang, X. J. Wei and G. W. Diao, *J. Phys. Chem. C*, 2013, **117**, 13593; (*b*) J. R. Krenn, *Nat. Mater.*, 2003, **2**, 210; (*c*) Y. Cao, R. Jin and C. Mirkin, *Science*, 2002, **297**, 1536; (*d*) A. R. Madaria, A. Kumar, F. N. Ishikawa and C. Zhou, *Nano Res.*, 2010, **3**, 564; (*e*) A. J. Haes and R. P. Van Duyne, *J. Am. Chem. Soc.*, 2002, **124**, 10596; (*f*) B. D. Moore, L. Stevenson, A. Watt, S. Flitsch, N. H. Turner, C. Cassidy and D. Graham, *Nat. Biotechnol.*, 2004, **22**, 1133.

11 (*a*) M. S. Goh, Y. H. Lee, S. Pedireddy, I. Y. Phang, W. W. Tjiu, J. M. R. Tan and X. Y. Ling, *Langmuir*, 2012, **28**, 14441; (*b*) A. Takai, Y. Doi, Y. Yamauchi and K. Kuroda, *J. Phys. Chem. C*, 2010, **114**, 7586; (*c*) Y. Sun and Y. Xia, *Adv. Mater.*, 2002, **14**, 833; (*d*) Y. Sun, B. Mayers, T. Herricks and Y. Xia, *Nano Lett.*, 2003, **3**, 955.

12 (*a*) W. K. Choi, T. H. Liew, M. K. Dawood, H. I. Smith, C. V. Thompson and M. H. Hong, *Nano Lett.*, 2008, **8**, 3799; (*b*) F. Kim, S. Kwan, J. Arkana and P. Yang, *J. Am. Chem. Soc.*, 2001, **123**, 4386; (*c*) Y. Huan, X. Duan, Q. Wei and C. M. Lieber, *Science*, 2001, **291**, 630; (*d*) N. A. Melosh, A. Boukai, F. Diana, B. Gerardot, A. Badolato, P. M. Petroff and J. R. Heath, *Science*, 2003, **300**, 112.

13 (*a*) X. Li, Y. F. Lim, K. Yao, F. E. H. Tay and K. H. Seah, *Chem. Mater.*, 2013, **25**, 524; (*b*) M. Tian, J. Wang, J. Kurtz, T. E. Mallouk and M. H. W. Chan, *Nano Lett.*, 2003, **3**, 919; (*c*) J. Yeon, Y. J. Lee, D. E. Yoo, K. J. Yoo, J. S. Kim, J. Lee, J. O. Lee, S. J. Choi, G. W. Yoon, D. W. Lee, G. S. Lee, H. C. Hwang and J. B. Yoon, *Nano Lett.*, 2013, **13**, 3978; (*d*) J. H. Park, P. Nagpal, K. M. Mcpeak, N. C. Lindquist, S. H. Oh and D. J. Norris, *ACS Appl. Mater. Interfaces*, 2013, **5**, 8701.

14 (*a*) M. Li, H. Schnablegger and S. Mann, *Nature*, 1999, **402**, 393; (*b*) X. Z. Zhou, Y. Zhou, J. C. Ku, C. Zhang and C. A. Mirkin, *ACS Nano*, 2014, **8**, 1511; (*c*) L. F. Xi, W. N. Xiu, W. Tan, C. Boothroyd and Y. M. Lam, *Chem. Mater.*, 2008, **20**, 5444; (*d*) Y. G. Li and Y. Y. Wu, *J. Am. Chem. Soc.*, 2009, **131**, 5851.

15 (*a*) C. Zhu, H. C. Peng, J. Zeng, J. Y. Liu, Z. Z. Gu and Y. N. Xia, *J. Am. Chem. Soc.*, 2012, **134**, 20234; (*b*) M. Ladanov, M. K. Ram, G. Matthews and A. Kumar, *Langmuir*, 2011, **27**, 9012; (*c*) S. W. Chou, J. J. Shyue, C. H. Chien, C. C. Chen, Y. Y. Chen and P. T. Chou, *Chem. Mater.*, 2012, **24**, 2527.

16 (*a*) Z. G. Chen, J. Zou, X. D. Yao, F. Li, X. L. Yuan, T. Sekiguchi, G. Q. Lu and H. M. Cheng, *Adv. Funct. Mater.*, 2008, **18**, 3063; (*b*) Y. W. Zhu, H. Z. Zhang, X. C. Sun, S. Q. Feng, J. Xu, Q. Zhao, B. Xiang, R. M. Wang and D. P. Yu, *Appl. Phys. Lett.*, 2003, **83**, 144; (*c*) R. C. Wang, C. P. Liu, J. L. Huang, S. J. Chen, Y. K. Tseng and S. C. Kung, *Appl. Phys. Lett.*, 2005, **87**, 013110.